A REVIEW OF THE 2023 ANTIPROTON PHYSICS RUN IN THE CERN ANTIMATTER FACTORY

L. Bojtár, B. Dupuy, Y. Dutheil, P. Freyermuth, D. Gamba,
L. Joergensen, B. Lefort, S. Pasinelli, L. Ponce
CERN, Geneva, Switzerland

Abstract

Despite a shorter-than-scheduled physics run due to a hardware problem, the AD/ELENA antiproton complex delivered record beam intensities to the experiments during the 2023 run. This paper reviews the performance of both the CERN Antiproton Decelerator (AD) and the Extra Low ENergy Antiproton (ELENA) decelerator and their associated transfer lines. It presents the main improvements that allowed these record beam intensities to be delivered to the experiments. Emphasis is put on the optimization of the injection line, progress made on the stochastic and electron cooling performance, increased deceleration efficiency and stability, and the software tools used. Remaining issues and potential future improvements for the coming run will also be presented.

INTRODUCTION

The Antiproton Decelerator (AD) at CERN has been serving users since 2000 with pbars. Initially, it provided a single 5.3 MeV bunch to three experiments. The beam time was shared, with each experiment running for 8 hours per day. To improve the availability and the number of captured antiprotons at the experiments a small ring, ELENA, was constructed and commissioned in 2018 [1, 2]. The Extra Low ENergy Antiproton (ELENA) decelerats the beam down to 100 keV. The ELENA project included the construction of new electrostatic transfer lines and a new extraction scheme. Two groups of transfer lines are connected to the ring as shown in Fig. 1. The first provides beam to the GBAR and PUMA experiments and the second to the AEGIS, ALPHA, ASACUSA 1/2, BASE, and STEP experiments. Up to four bunches are ejected on each cycle to one or both groups of transfer lines. The bunches are distributed further to the experiments using fast deflectors in the transfer lines. The distribution of bunches is coordinated by a real-time beam request server. This is great progress compared to the single-bunch ejection scheme of the AD. AD and ELENA is operated 24h, 7 days a week for about 8 months/year.

ELENA also has a local H- source [3] foreseen initially for commissioning purposes, but which is now regularly used for machine developments, setup, and testing. The H- source stability has been greatly improved since its installation. A big advantage of using the H- source is the higher repetition rate, at around one shot per 12 seconds, instead of the 2 minute cycle required with pbars.

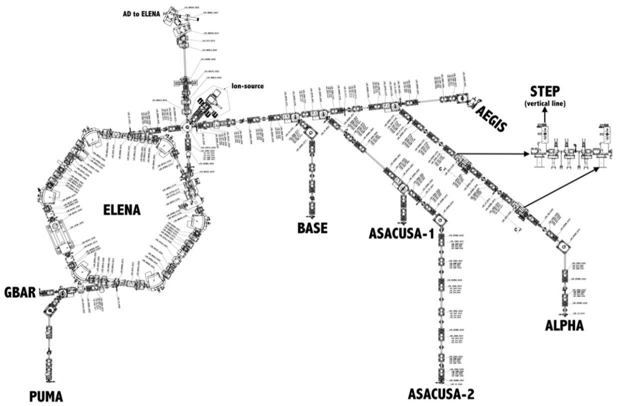

Figure 1: ELENA ring with the extraction lines.

AD AND ELENA DECELERATION CYCLES

The AD deceleration cycle is 109 seconds long and has 4 stages of beam cooling as shown in Fig. 2. The beam is produced on an iridium target through the impact of a 26 GeV/c proton beam coming from the Proton Synchrotron in 5 bunches. Antiprotons are collected with a magnetic horn and filtered by a curved part of the injection line, called the "dogleg". The AD ring has a big acceptance in all planes to keep a large portion of the incoming antiprotons. After injection, the beam is immediately rotated longitudinally by two 500 kV, 10 MHz cavities at harmonic 6. The momentum spread is reduced from the 3 % ring acceptance to the 1.7 % acceptance of the stochastic cooling. At the 3.57 GeV/c injection flattop and 2 GeV/c flattop stochastic cooling is used. Further down in the cycle electron cooling is applied at 300 MeV/c and 100 MeV/c. After Long Shutdown 2 (LS2) between 2019-2021, it was found that a mixed cooling at 100 MeV/c gives better transfer profiles and shorter bunches. First, a coasting beam is cooled, then the beam is bunched and cooled further for 2 seconds.

The AD operates with two optics. The optics change takes place after the second stochastic cooling. The main parameters of the AD are summarized in Table 1.

The ELENA cycle is shorter, only 12 seconds long. It has two stages of electron cooling at 35 MeV/c and 13.7 MeV/c. It is constructed such that the same magnetic cycle can be used with H-. This allows the operation team to set up the pbar cycle with the local H- source, which has a much higher repetition rate than the AD. H- injection takes place on the plateau at 13.7 MeV/c at the beginning of the ELENA cycle shown in Fig. 3. During normal operation with pbars there is

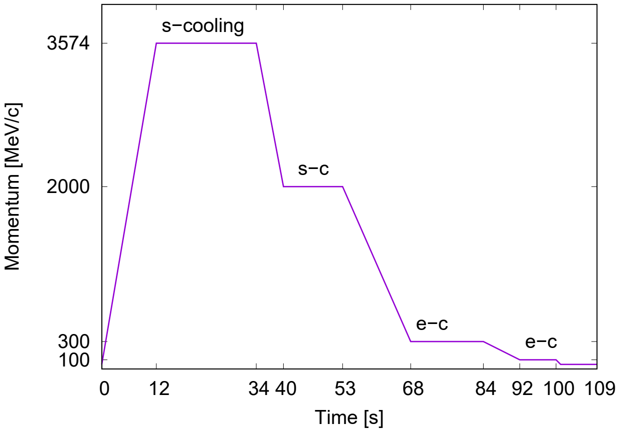

Figure 2: The AD deceleration cycle.

no H- injection at the beginning of the cycle. As the ELENA cycles are shorter than the AD cycle, dedicated H- cycles can be interleaved between the operational pbar cycles.

Table 1: AD Main Parameters

Parameter	Value
Circumference [m]	182
Prod. beam [protons/cycle]	1.9×10^{13}
Injected beam [pbars/cycle]	4.5×10^{7}
Momentum [GeV/c]	3.57-0.1
$1\sigma\epsilon_{tr}$ [μm]	30-0.9
±dp/p	$3 \times 10^{-2} - 10^{-4}$
Cycle length [s]	109
Dec. efficiency [%]	90
High energy tunes	$Q_h = 5.39$, $Q_v = 5.37$
Low energy tunes	$Q_h = 5.46$, $Q_v = 5.42$

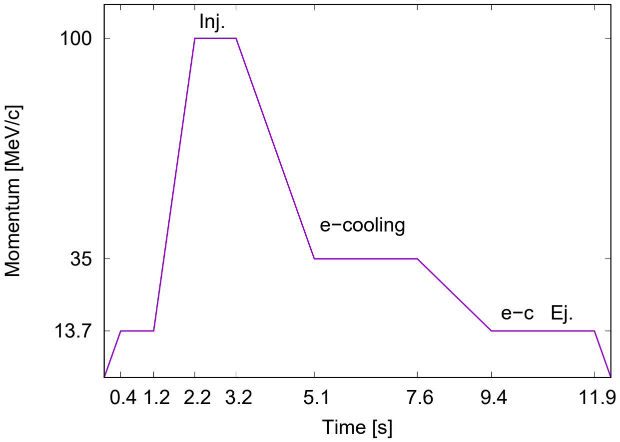

Figure 3: The ELENA deceleration cycle.

OPERATION AND 2023 RUN

The 2023 run was shorter than scheduled due to a water leak on a quadrupole, which delayed the start by two months to June. The run ended in November. During the year the ejected intensity from ELENA increased steadily until a fault of the magnetic horn, where a loose mechanical connection limited the operating voltage for the remainder of the year to 5 kV compared to the nominal 6.5 kV. This trend of increasing intensity is visible in Fig. 4, where the drop due to the horn fault is also seen.

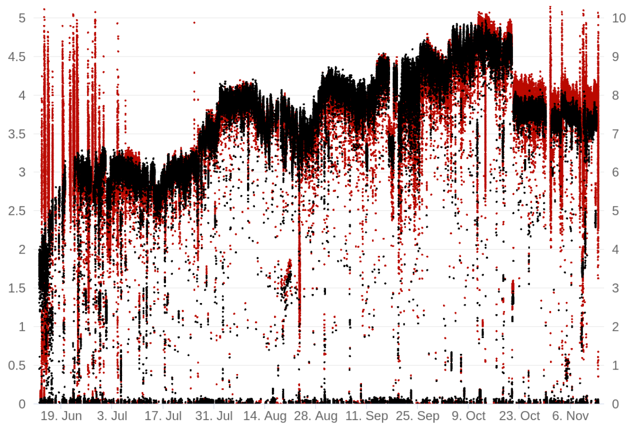

Figure 4: Ejected intensity from AD and ELENA throughout the 2023 run. The black dots are ejection intensities from the AD in units of 10^7 pbars belonging to the left scale. The red dots are ejected intensities/bunch from ELENA in units of 10^6 pbars belonging to the right scale.

The number of pbars extracted from the ELENA ring as a function of protons on target is shown in Fig. 5. Data from a few weeks period of 2022 operation is compared to data from 2023. There were several factors contributing to the intensity increase that can be observed.

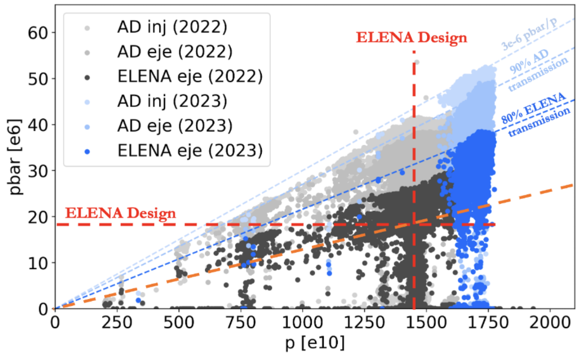

Figure 5: Antiproton intensity as a function of protons on the AD target. Pbars measured at AD injection, ELENA injection, and ELENA extraction are indicated from lighter to darker colors respectively. Shades of black and blue indicate 2022 and 2023 data, respectively. Proton on target and ELENA extraction design parameters are also indicated in dashed red.

In the AEGIS zone, additional shielding blocks have been installed to reduce the radiation level in the AD hall. This allowed an increase in the production beam intensity and took advantage of the possibility to produce 5 production beam bunches. New software has been developed to stabilize the production beam as it tended to drift slowly with time so that the beam position on the target had to be readjusted. This is done now automatically by a beam stabilizer software running continuously in the background.

The stochastic cooling also got an upgrade. The notch filter was changed from a mechanical trombone to an optical delay line for the 3.57 GeV/c signal path. It is now less temperature dependent [4]. In the past, the delays had to be readjusted when the outside temperature changed significantly. This was not an issue during 2023.

Tune and orbit have been adjusted all along the AD and ELENA cycles to minimize the losses. Optimization of the stochastic cooling and alignment of the electron cooling also contributed to the improvements in both machines.

Table 2 compares the main parameters of ELENA to the design values. One can see that the beam intensity and deceleration efficiency exceed the design values. The beam emittances are higher than the design values in all planes. This is somewhat related to the higher-than-foreseen intensity. It was already known in the design phase of ELENA that the tune shift due to space-charge and intra-beam scattering is likely to put a limitation on the ELENA intensity. These effects are visible through the reduction in the ejected emittances when occasionally receiving lower-intensity production beam shots.

Table 2: Comparison of the ELENA Design Parameters with the Average 2023 Values

Parameter	Design value	2023 value
Injected pbars	3×10^7	4×10^7
Ejected pbars	1.8×10^7	3.2×10^7
Dec. efficiency [%]	60	80
RMS Bunch length [ns]	75	100
Ejected $1\sigma\epsilon_h$ [μm]	1.2	2
Ejected $1\sigma\epsilon_v$ [μm]	0.75	2
±dp/p	5×10^{-4}	1.3×10^{-3}

The working point of ELENA used during the 2023 run was the same as used during the commissioning $Q_h = 2.375$, $Q_v = 1.39$. This working point, however, led to bigger transverse emittances than the design value. Since the emittances are intensity dependent [5], it was suspected that the defocusing effect of space charge pushes particles in the distribution to lower values and those particles hit the third-order resonance line. A new working point has been tested and put in place with tunes $Q_h = 2.285$, $Q_v = 1.31$ which is below the third order resonance line. This working point gives about 2 times smaller transverse emittances. During the 2024 re-start, the ELENA cycle was optimized with this new working point.

Continual improvements to the beam instrumentation of ELENA also contributed to the performance. The Schottky signal is an important tool for the setup of the electron cooler and is derived from the combined signals of all ring pickups of the orbit system [6]. Extensive work was carried out on the characterization and improvement of the scraper system [7] for transverse beam size measurements, and the Secondary Emission Monitors (SEM) in the ELENA lines remain essential instruments for operation, for example for measuring the transport line Twiss parameters using several SEM inserted into the beam at the same time.

The main equipment faults are summarized in Table 3. ELENA had very few issues. The majority of faults were due to the injector chain or aging equipment in the AD.

Table 3: Major Source of Downtime

Fault cause	Duration [h]
Injector complex	378
Power supplies	42
Radiofrequency	5
Magnetic horn	6
Other	11

CONCLUSIONS

Various improvements during the 2023 run led to record intensities delivered to the experiments. These included adding shielding to reduce radiation levels in the AD hall allowing higher production beam intensities, software to stabilize position fluctuations on the target, a new working point in ELENA, a more stable notch filter for the stochastic cooling, better instrumentation, and optimizations along the deceleration cycles. Excluding the delay caused by the fault on a quadrupole at the start of the run, and upstream faults in the injector complex, AD/ELENA had a remarkable 97.5 % availability in 2023.

ACKNOWLEDGEMENTS

The authors would like to thank all their colleagues from the equipment groups for their continuous support during the commissioning and operation of the AD-ELENA complex.

REFERENCES

[1] V. Chohan *et al.*, *Extra Low ENergy Antiproton (ELENA) ring and its Transfer Lines: Design Report*. CERN, 2014.

[2] T. Eriksson *et al.*, “ELENA – from installation to commissioning”, in *Proc. of IPAC’17*, Copenhagen, Denmark, 2017, pp. 3327–3330. `doi:10.18429/JACoW-IPAC2017-WEPVA034`

[3] A. Megía-Macías, R. Gebel, and B. Lefort, “The ion source for the commissioning of ELENA ring”, *AIP Conf. Proc.*, vol. 2011, no. 1, p. 090 014, 2018. `doi:10.1063/1.5053395`

[4] S. Rey *et al.*, “Experience with Beam Transfer Function Measurements for Setting-up the Stochastic Cooling System in the CERN Anti-Proton Decelerator (AD)”, *Proc. COOL’23*, 2024, accepted and to be published under `doi:10.18429/JACoW-COOL2023-THPOSRP22`.

[5] D. Gamba, F. Asvesta, P. Kruyt, L. Ponce, and G. Russo, “Status of E-Cooling Characterisation at 100 keV in ELENA”, *Proc. COOL’23*, 2024, accepted and to be published under `doi:10.18429/JACoW-COOL2023-THPAM1R3`.

[6] O. Marqversen and S. Jensen, “Schottky Signal From Distributed Orbit Pick-Ups.”, in *Proc. IBIC’21*, 2021, pp. 366–369. `doi:10.18429/JACoW-IBIC2021-WEPP04`

[7] G. Russo, B. Dupuy, D. Gamba, and L. Ponce, “Transverse Emittance Reconstruction Along the Cycle of the CERN Antiproton Decelerator”, in *Proc. HB’23*, Geneva, Switzerland, Oct. 9–13, 2023, 2024, pp. 358–362. `doi:10.18429/JACoW-HB2023-THC1C1`